Hindawi
Shock and Vibration
Volume 2022, Article ID 3235063, 11 pages
https://doi.org/10.1155/2022/3235063

Research Article

Strata Caving and Gob Evolution Characteristic in Longwall Mining

Weidong Pan,[1,2] Xinyuan Li ,[1,2] and Zhining Zhao[1,2]

[1]*School of Energy and Mining Engineering, China University of Mining and Technology, Ding No. 11, Xueyuan Road, Haidian District, Beijing, China*
[2]*State Key Laboratory of Coal Resources and Safe Mining, China University of Mining and Technology, Ding No. 11, Xueyuan Road, Haidian District, Beijing, China*

Correspondence should be addressed to Xinyuan Li; xli82@lakeheadu.ca

Received 22 December 2021; Accepted 24 February 2022; Published 20 March 2022

Academic Editor: Zhanbo Cheng

It is usually difficult to capture strata caving and gob evolution characteristic in longwall mining at engineering scales. This paper uses bonded block modelling (BBM) approach within a distinct element method (DEM) code to simulate strata behaviour in longwall mining, which captures the caving phenomena and bulking characteristics of roof strata successfully. Many features in longwall mining, including the caving and compaction of gob strata and the associated stress evolution, are reproduced in the model. Four zones in longwall gob are identified based on its stress characteristics: voussoir influencing zone, compacted zone, compacting zone, and pilling zone. The initial bulking factor of the caved strata ranges from 1.12 to 1.25 and decreases gradually to the residual bulk factor of approximately 1.05 as the longwall face advances. The caved strata in the longwall gob present strain hardening behaviour and the load carrying capacity increases exponentially as a function of strain. Moreover, the range of the interaction between the caving strata and the overburden in gob was discussed, which provides a reference when using a continuum method to simulate longwall mining.

1. Introduction

Longwall mining is a widely used underground coal extraction method for its high production and recovery rate. After coal seam excavating, the strata above the coal seam are destressed and fractured as it is subjected to excavation disturbances [1]. As the working face advances, the roof strata gradually collapse and cave into the mined-out area until the uncaved strata are in contact with the caved one [2]. There are three zones above the gob based on the degree of strata failure and crack development in the overburden strata, as illustrated in Figure 1: caved zone, fractured zone, and continuous deformation zone in ascending order from the roofline [3].

To capture the weighting law and ensure the stability of hydraulic supports, many of significant researches have been done on the structural characteristics of the overlying strata [4–9]. These works demonstrate that force-transmitting structure exists in fractured zone, which can bear the load exerted by the upward strata, and the associated instability of these structures may result in the weighting of the working face. However, the caved zone and its status were neglected to some extent. As the longwall face continuously advances, the broken rock in the caved zone is gradually compacted under the effects of self-weight and the load exerted from the overlying strata, and the pore structure and arrangement of collapsed rock change constantly. These can affect the surface subsidence, greenhouse gas underground storage, spontaneous combustion of underground residual coal, underground reservoir construction, water resource filtration, gob gas-outing, and abandoned mine use [10]. In addition, a significant amount of gas and water accumulate in the caved zone owing to its high porosity and permeability, making it challenging to ensure safe production [11, 12]. Therefore, it has received increasing attention in recent years.

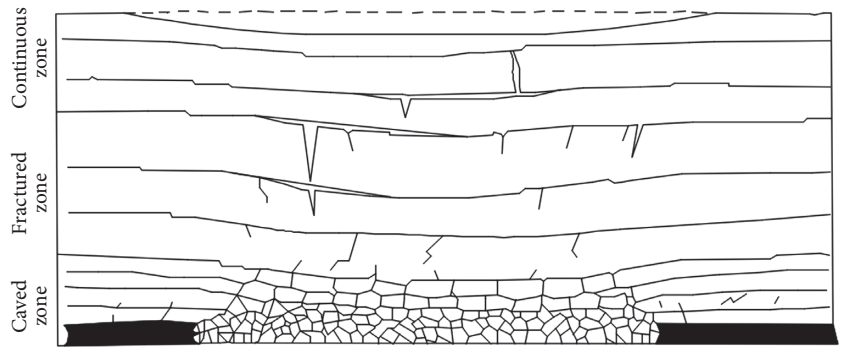

Figure 1: Three key disturbed zones above the longwall panel due to longwall mining.

The caved strata, as a kind of bulk material, changes continually with the compaction effect from the overlying strata, such as density, modulus, Poisson ratio, stress, strain, porosity, permeability, and even stress distribution. Many significant researches have been conducted on the evolution of the gob [13–16]. However, these researches mostly focus on a sample-scale experiment, which have some differences with the field condition, such as specimen size and boundary condition, and the monitoring means are limited. Therefore, it is significative to reproduce the gob compaction process explicitly considering for the mining activities at engineering scales. Numerical methods provide an effective approach to capture these features.

The numerical methods can be classified into continuum methods (such as boundary element method (BEM), finite element method (FEM), finite-difference method (FDM)), and discontinuum methods (such as distinct element method (DEM) and discontinuous deformation analysis (DDA)) and hybrid methods (such as FEM/DEM and FDM/DEM) [17, 18]. Continuum methods have been used to simulate longwall mining for decades but have impactful limitations. These methods cannot realize the generation and propagation of fractures; therefore, the fracturing and caving processes of strata cannot be readily captured explicitly. In contrast, discontinuum methods are more appropriate to simulate fracturing and caving of strata as caused by longwall mining.

In this paper, an engineering scale numerical model was established using the Universal Distinct Element Code (UDEC) with a proposed bonded block modelling approach. This approach considers both preexisting discontinuity and fictitious contact. The progressive caving of the roof strata and gob evolution are then investigated, and the range of the interaction between the caving strata and the overburden in gob was discussed, which could provide a reference when using a continuum method to simulate longwall mining.

2. DEM Model of Longwall Mining

The two-dimensional UDEC program was used to develop a field-scale longwall model in this paper. The UDEC code can explicitly model large-scale movement of overlying strata and the complete detachment and rotation of collapsed rock. In longwall mining, the advancement of the face along the panel length is much greater than along the panel width. Hence, a UDEC model with plane-strain conditions, which represents the longwall face advancing along the panel length and located at the mid-panel width, can identify fundamental rock responses caused by longwall mining [19].

2.1. Bonded Block Modelling Approach. In the bonded block model (BBM), rock strata and coal seam are represented as an assembly of polygonal blocks bonded together through "contacts" in a fictitious contact position, as shown in Figure 2. Each block is considered to be elastic-plastic by dividing it into triangular finite-difference zones. Failure can occur both in the zones and the fictitious contact through shear or tension, depending on the stress state and mechanical properties. However, the fracturing can only occur in the fictitious contact.

In the direction normal to fictitious contact, the stress-displacement relationship is assumed to be linear and governed by the stiffness k_{n} as [20],

$$\Delta\sigma_{\mathrm{n}} = -k_n \Delta u_n, \tag{1}$$

where $\Delta\sigma_{\mathrm{n}}$ is the effective normal stress increment and Δu_{n} is the normal displacement increment. There is a limiting tensile strength, T, for the contact. If the tensile strength is exceeded, then $\sigma_n = 0$.

In the shear direction, the response is governed by a constant shear stiffness, and the shear stress, τ_s, is determined from a combination of the contact microproperties; namely, cohesive (C) and frictional (φ). Thus, if [20]

$$\left|\tau_s\right| \le C + \sigma_n \tan\varphi = \tau_{\max}, \tag{2}$$

then

$$\Delta\tau_s = -k_s \Delta u_s, \tag{3}$$

or else, if

$$\left|\tau_s\right| \ge \tau_{\max}, \tag{4}$$

then

$$\tau_s = \mathrm{sign}\left(\Delta u_s\right)\tau_{\max}, \tag{5}$$

where Δu_s is the incremental shear displacement.

By using the BBM, rock strata and coal seam are discretized into several smaller-sized blocks with hexagonal

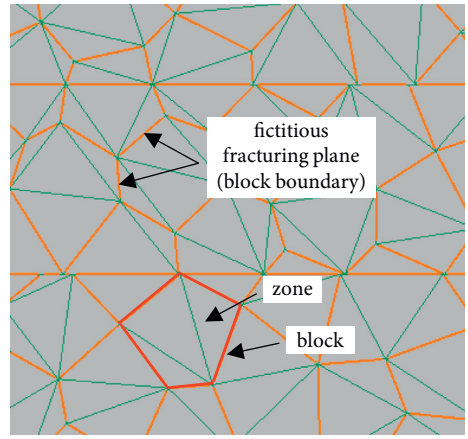

Figure 2: Element of a bonded block model.

shapes. Thus, fracturing of the roof strata can be realistically simulated, and the roof strata can spontaneously collapse and cave into the gob to sufficiently model the roof caving process, which can reappear the process of roof breaking and caving in longwall mining.

2.2. Model Configuration. The current model is based on a panel of the Tashan coal mine, which is part of the China Coal Group, in Shanxi province, China. The longwall panel is located at a depth of approximately 430 m, which has a width of 240 m and length of 2000 m. The mined coal seam has an average thickness of 3.0 m and is inclined at an angle of 0–8°.

The longwall model was created using the bonded block modelling approach, as shown in Figure 3, with 300 m wide and 120 m high, and simulates the longitudinal section through the initial stage of panel extraction. The comprehensive histogram of the rock strata is shown in Figure 3(b). To improve the computational efficiency, only the rock strata in potential breaking and caving range are discretized into hexagonal block, and rock strata above this range are not discretized. The strata below the seam are discretized into coarse rectangular blocks. The block size in potential caving range is 1.0 m, which is sufficient to simulate the fracture and caving behaviours of roof strata [17]. Two 70 m wide pillars are left on both sides of the panel. The horizontal displacement is restrained on the left and right model boundaries and both vertical and horizontal displacements are fixed at the base. A vertical stress of 8.7 MPa is applied on the top boundary and is equal to the overburden. The Mohr–Coulomb yield criterion is used to describe the behaviour of the blocks, and the parameters used in this model are shown in Table 1.

The bedding planes between the rock layers are simulated using horizontal persistent joints. Other preexisting discontinuities, including horizontal and vertical joints, are randomly incorporated in the roof strata, as shown in Figure 3(c). The cohesion and tensile strength of these preexisting discontinuities are assumed to be zero and the friction angle is assumed to be 30 [17], and the fictitious contact between the hexagonal blocks has an equal strength with the block but can be destroyed. The stiffness of the fictitious contact is set according to (6) and experience and determined by inversion. The detail parameters of the contact are shown in Table 2.

$$K_n \text{ or } K_s = (1 - 10) \times \frac{(K + 4/3G)}{z}, \tag{6}$$

where K and G are the bulk and shear modulus, respectively, and z is the smallest width of an adjoining zone in the normal direction.

A series of monitoring points at different positions are set to capture the compaction characteristics of caved strata in longwall gob, as shown in Figure 4. These monitoring points play different roles, including displacement and stress monitoring points to obtain the strain and stress of the compacted zone, respectively. Thus, the monitoring results from all eight positions are provided. The bulk factor is obtained from thickness after caving divided by the initial thickness and the strain is obtained from thickness changes in the caved strata divided by the initial thickness before strata caving. The stress in the gob floor is measured, which is used to represent the gob stress.

The advance of the longwall is simulated from the left to the right side of the model using a stepwise excavation with a 10 m long advancing distance. After each stepwise excavation, the timesteps are processed until the caving of strata completes and the model reaches a relatively stable state.

3. Numerical Simulation Results

3.1. Caving Process of Roof Strata. Figure 5 shows the progressive caving process of the roof strata during the longwall advance. When the longwall advances 20 m, some macroscopic fractures are generated in the immediate roof with an approximately 3 m deep extending distance. Thus, some of the rock blocks in the first layer fail and cave due to their lower strength (Figure 5(a)). As the face advances to 40 m, more fractures are generated and extended to the entire immediate roof, which behaves as a soil-like material and caves into the gob area of the arch range below the main roof (Figure 5(b)). As the longwall continues to advance, the main roof behaves as a beam and caves, and the strata above

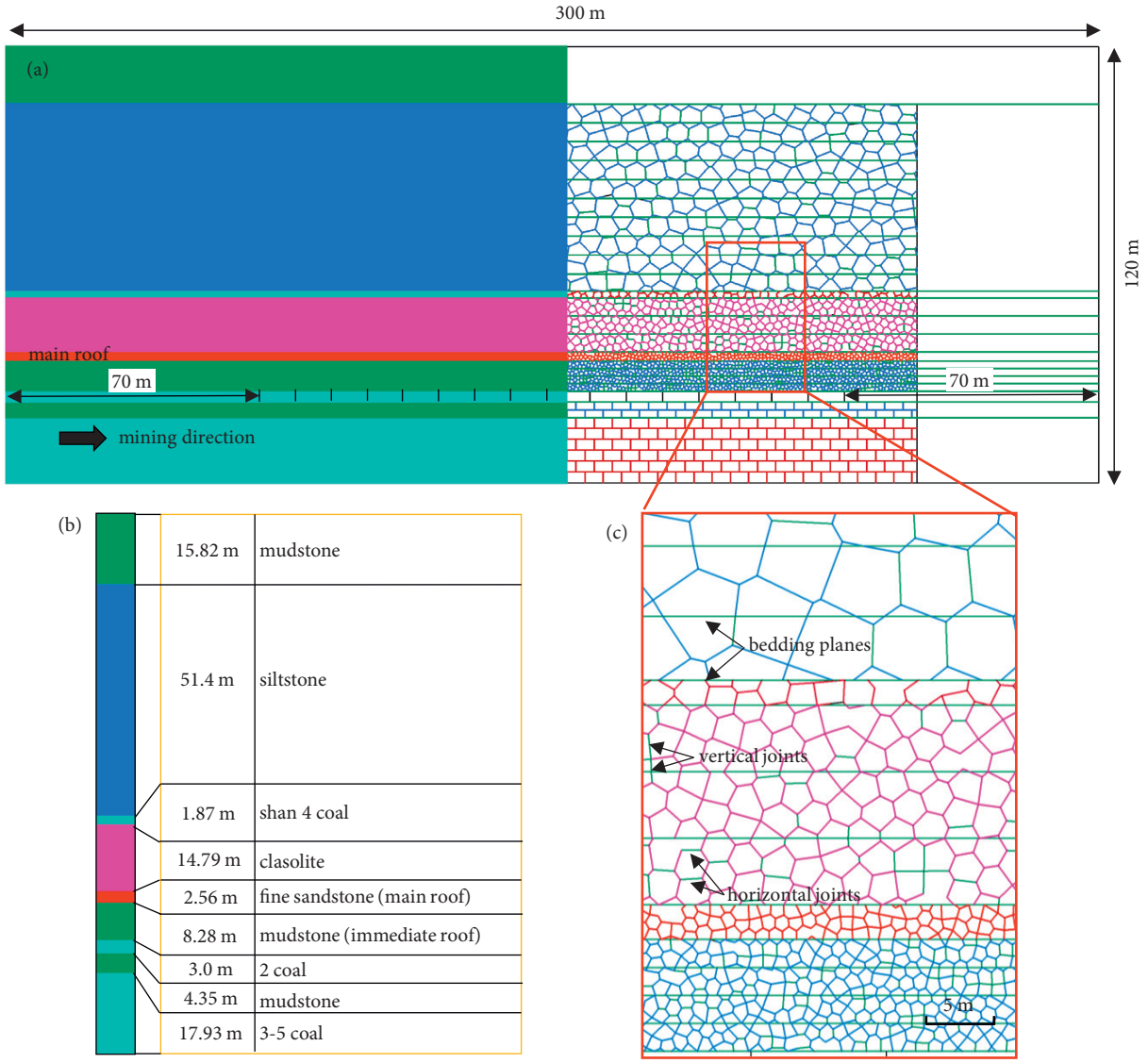

Figure 3: Configuration of the longwall model using the UDEC BBM approach.

Table 1: Properties of coal and rock block in the BBM.

Lithology	Density (kg/m^3)	E (GPa)	ν	C (MPa)	φ (°)	σ_t (MPa)
Mudstone	2570	5.12	0.36	1.38	34.90	0.43
Siltstone	2610	6.14	0.20	1.60	38.57	0.84
Coal	1360	1.05	0.36	0.36	34.45	0.23
Clasolite	2640	2.07	0.22	1.27	38.10	0.40
Fine sandstone	2530	13.48	0.15	2.84	35.89	2.03
Mudstone	2570	5.12	0.26	1.38	34.90	0.43
Coal (excavation)	1360	1.05	0.36	0.36	34.45	0.23
Mudstone	2570	5.12	0.26	1.38	34.90	0.43
Coal	1360	1.05	0.36	0.36	34.45	0.23

it caves simultaneously. Meanwhile, bed separation appears with a range larger than 10 times the mining height (Figure 5(c)). As the longwall advances to 80 m, the main roof caves at the second time (Figure 5(d)), and the bed separation continues to develop upwards. When the face advances to 100 m, strata movement develops continually while the bed separation begins to close-up due to the compaction of the upward strata movement (Figure 5(e)). However, some vertical fractures begin to appear in the upper strata at the edge of the gob. In this stage, the caved material in the gob is gradually compressed by the overlying strata. As the longwall continues to advance, the main roof

Table 2: Contact properties in the BBM.

Discontinuity		K_n (GPa/m)	K_s (GPa/m)	C (MPa)	φ (°)	σ_t (MPa)
Fictitious contact	Siltstone	11.37	11.37	1.38	38.57	0.84
	Coal	4.39	4.39	0.36	34.45	0.23
	Clasolite	5.91	5.91	1.27	38.10	0.40
	Fine sandstone	35.57	35.57	2.48	35.89	2.03
	Mudstone	41.79	41.79	1.38	34.90	0.43
	Coal (mining)	20.89	20.89	1.38	34.90	0.43
	Mudstone	5.85	5.85	0.36	34.45	0.23
Joints		50	25	0	30.0	0

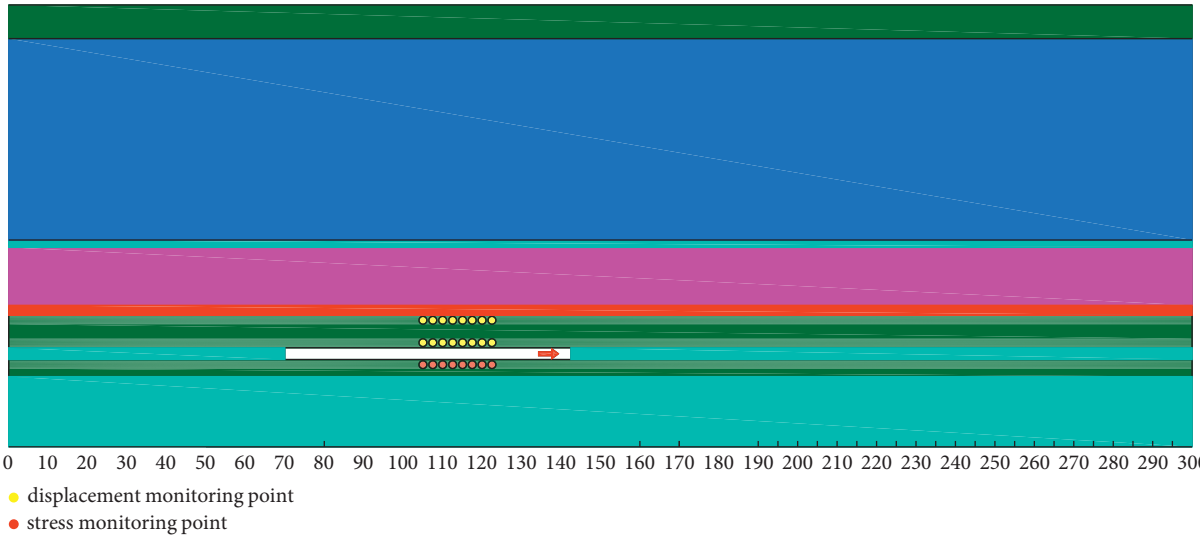

Figure 4: Arrangement of monitoring points.

caves periodically, and the caved strata are constantly compressed, as shown in Figures 5(f)–5(h). In the numerical model, the initial and periodical caving distance is 55 m (advancing distance minus opening width) and 20 m, respectively, which have a good consistency with the field data (48 m and 23 m) and prove the rationality of the numerical model in some extent.

Figure 6 is a magnified image of the final state of the overlying strata movement corresponding to stage 8 from Figure 5(h). Three distinct zones (caved, fractured, and continuous) are realistically captured in the proposed model. The strata in the caved zone collapsed and caved into the gob and piled irregularly with a high porosity, while the strata in the fractured zone are characterized by the cracks along different directions. There are large horizontal and vertical displacements in the sides of the gob; however, the displacement is mainly consisted of vertical one in the middle position of the gob. Therefore, the cracks at both sides of the gob are longitudinally distributed while cracks in the middle of the gob are laterally distributed, which is caused by the differential vertical displacements.

3.2. Stress Evolution in Longwall Gob. The extraction of the coal seam and the movement of the roof strata cause stress redistribution around the mined-out area. The vertical and horizontal stress distributions around the mined-out area at different mining stages are shown in Figures 7 and 8. The extraction of the coal results in a vertical stress concentration for the two sides of the mined-out area as the horizontal stress decreases. The rear and front abutment stresses gradually increase as the longwall advances, and the horizontal stress remains relatively stable and does not change with the longwall advancement. However, this state is broken when the collapsed strata in the caved zone contacts the uncaved strata. Both the vertical and horizontal stresses around and in the mined-out areas start to decrease because of the bearing capacity coming from the caved strata in gob, as shown in Figures 7(e) and 8(e). Crushing and compacting of the caved strata change the void distribution and cause further changes in the stress state in the gob as the longwall continues to advance. Nevertheless, the distribution of the rebalanced stress is never uniform due to the inhomogeneity of the caved strata as whole, as shown in Figures 7(f)–7(h) and Figures 8(f)–8(h).

Based on the stress evolution characteristics, four zones may exist in the gob along the direction of longwall advance, as shown in Figure 6: (i) voussoir influencing, (ii) compacted, (iii) compacting, and (iv) pilling zones. The voussoir influencing zone is under the voussoir beam located at the back of the longwall gob, which is formed by the key block of the broken main roof. In this zone, the stress is relatively

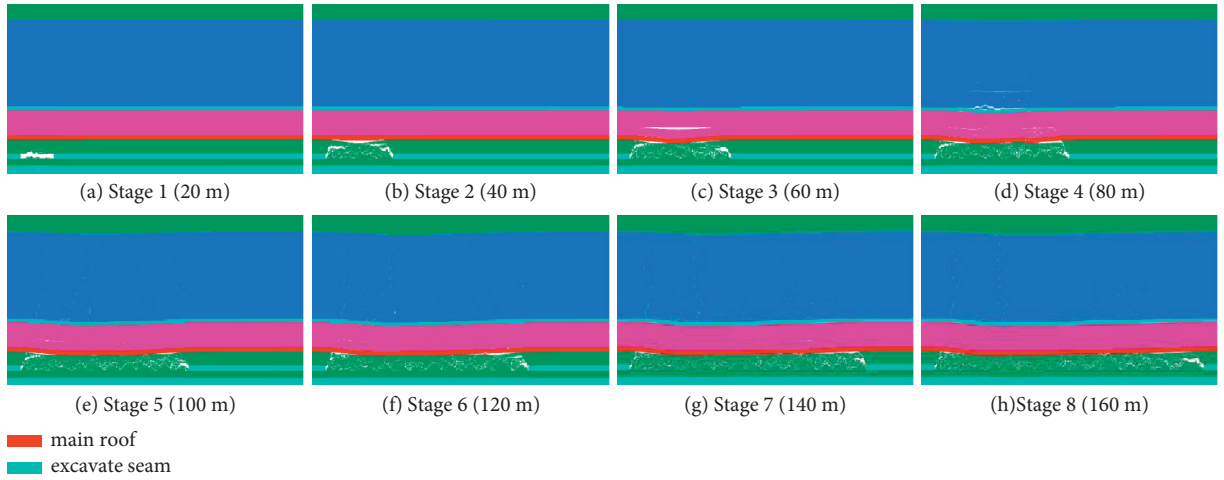

Figure 5: Progressive caving of the overlying strata during the longwall advance. (a) Stage 1 (20 m). (b) Stage 2 (40 m). (c) Stage 5 (60 m). (d) Stage 4 (80 m). (e) Stage 5 (100 m). (f) Stage 6 (120 m). (g) Stage 7 (140 m). (h) Stage 8 (160 m).

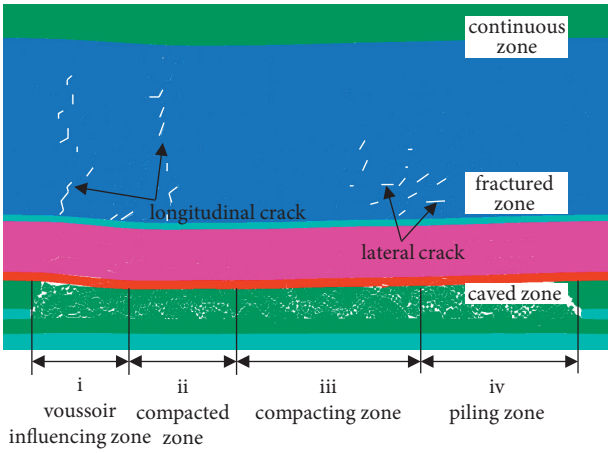

Figure 6: Zones in gob and overlying strata caused by longwall mining.

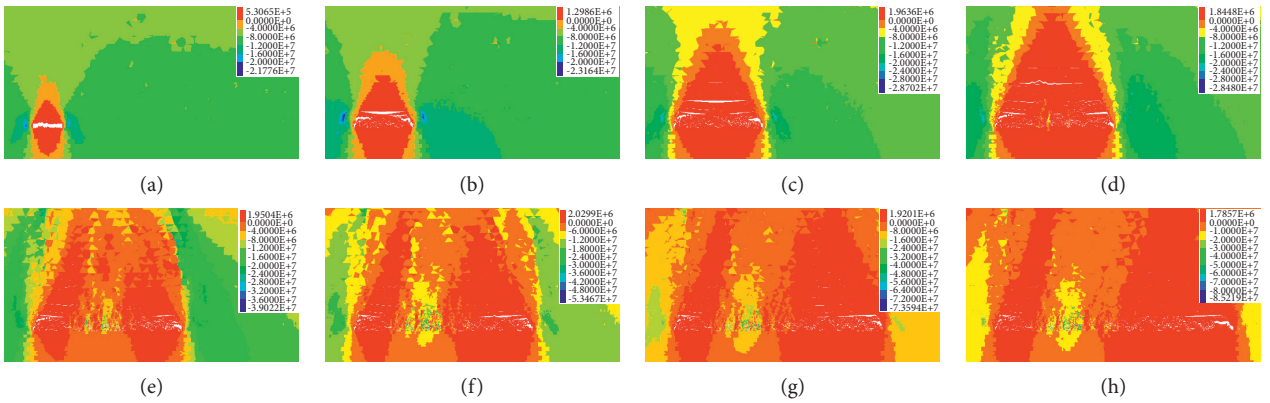

Figure 7: Vertical stress distributions around the mined-out area. (a) Stage 1 (20 m). (b) Stage 2 (40 m). (c) Stage 5 (60 m). (d) Stage 4 (80 m). (e) Stage 5 (100 m). (f) Stage 6 (120 m). (g) Stage 7 (140 m). (h) Stage 8 (160 m).

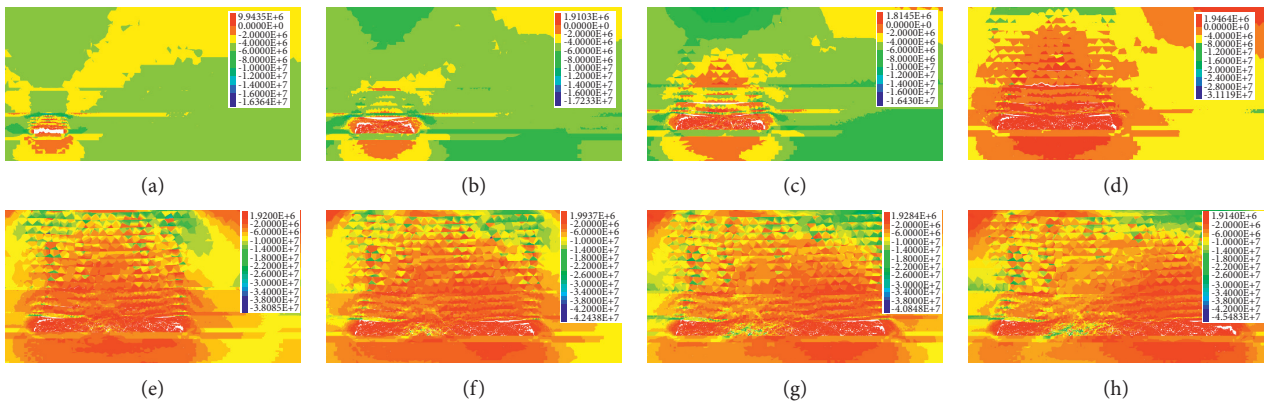

Figure 8: Horizontal stress distributions around the mined-out area. (a) Stage 1 (20 m). (b) Stage 2 (40 m). (c) Stage 5 (60 m). (d) Stage 4 (80 m). (e) Stage 5 (100 m). (f) Stage 6 (120 m). (g) Stage 7 (140 m). (h) Stage 8 (160 m).

small, and the caved strata are less compacted; therefore, the porosity and void fraction are large. In the compacted zone, the caved strata are compacted by the uncaved strata and the stress is higher. The caved strata in the compacting zone are been compacted, while caved strata in the pilling zone are heaped up irregularly and have a large gap with the uncaved strata.

Figure 9 shows the final stress distribution on the floor of the longwall gob. The vertical stress in the compacted zone is larger than the premining stress, which demonstrates that the compacted zone bears its own overburden as well as the overburden adjacent to it. The vertical stresses in the other zones are smaller than the premining stress and present a contrary tendency along both sides of the compacted zone. The vertical stress in the voussoir influencing zone overall increases with the distance from the left mining boundary but decreases slightly near the mining boundary due to stress concentration on the boundary coal pillar. The vertical stress in compacting zone decreases gradually with the distance from the compacted zone, which implies the strain of the caved strata decreases gradually and the caved rock strata have been compacting. The vertical stress distribution in the pilling zone is relatively uniform and approaches the weight of the caved strata, which indicates that the caved strata are not in contact with the uncaved strata and there is no stress transfer path between them. However, the horizontal stress presents different characteristics. In the voussoir influencing and pilling zones, the horizontal stress is near the premining stress, and it returns to the state of premining stress in the compacted zone, although in a nonuniform form, but it is relatively small in the compacting zone.

Although with a specific trend, the stress on the floor of the longwall gob has a sharp jagged shape. This may be related to the force transferring path in the caved strata. As a kind of bulk material, the force in caved rock strata transfers from the force chain, which causes an inhomogeneous stress distribution, as shown in Figure 10. This introduces a sporadic contact force that can be relatively large due to the stress concentration.

3.3. Compaction Characteristics of the Longwall Gob. The evolution of the bulk factor objectively reflects changes in the porosity of the caved strata. The evolution of the bulk factor with the longwall advance in the eight regions is seen in Figure 11. Although there are various initial bulk factors in the different regions, in general, it ranged from 1.12–1.25, except for the regions of $x = 110$ m. This exception is strongly related to the caving state of the roof strata. The bulk factor is relatively large when the size of the caved rock strata is small, while the value would be small. The range of the initial bulk factor is corresponded to the caved zone range of 4–8 times the mining height; thus, it is widely used to estimate the height of the caved zone. The bulk factor decreases gradually with the longwall advance but at a reducing rate and tends to be stable after the working face advances 60 m. The residual bulk factor is around 1.05.

Figure 12 shows the stress-strain relationship at different positions along the longwall gob. The stress-strain relationship varies with position but possesses a strain hardening behaviour that increases exponentially, which indicates that the pore structure between blocks diminishes with the longwall advance. For all eight monitoring points, the stress-strain curves at $x = 105$, 107.5, 115, 120, and 122.5 m are similar in terms of their increasing trends and growth process, while the other curves increase either faster or slower. This may be related to the force chain transferring characteristics in caved strata. In general, the stress-strain response of caved material is analogous with the work conducted by Pappas and Mark [13].

4. Determination of the Range of Compacted and Compacting Zones

The continuum method is widely used to simulate the longwall mining issue due to its increased computational efficiency. However, this method cannot reflect the mechanical response of the gob automatically, which puts some limits on the use of this method. Therefore, a filling method is usually used to simulate the mechanical response of the

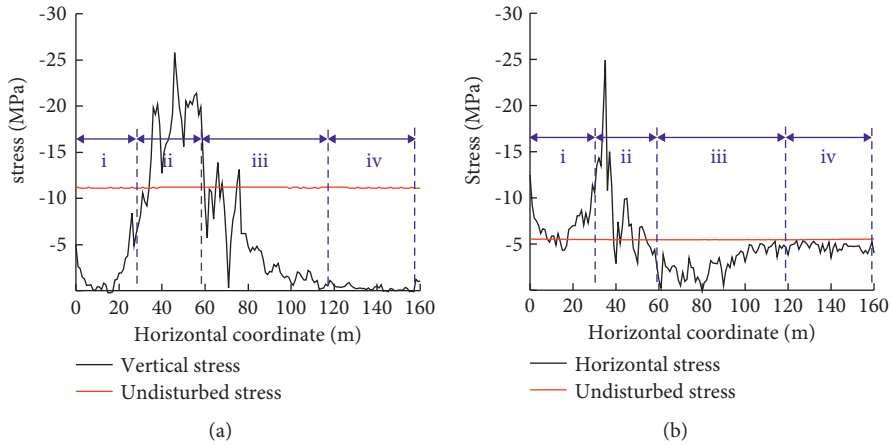

Figure 9: Final stress distribution in the longwall gob: (a) vertical stress and (b) horizontal stress and (i) voussoir influencing zone; (ii) compacted zone; (iii) compacting zone; and (iv) pilling zone.

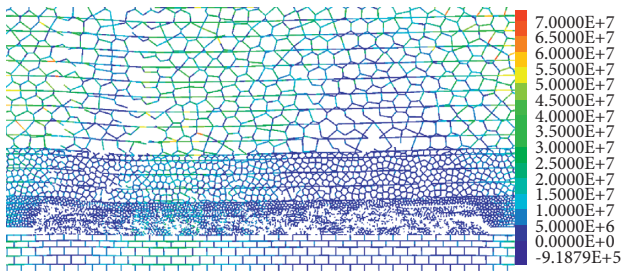

Figure 10: Contact force between blocks in longwall mining.

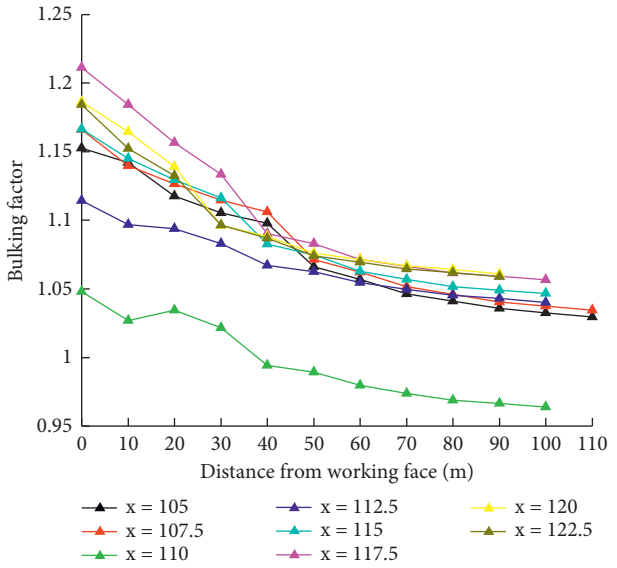

Figure 11: Evolution of the bulk factor with the longwall advance.

gob [21–24], and there are two caveats when using this method in longwall mining: (i) the constitutive model for gob modelling and (ii) the refilling range. As for the constitutive model, the double-yield model has been widely used and was proved to have a good relation with the reality [23, 25, 26]. So, it is of great importance to determine the actual range of the interaction between the caving strata and the overburden in gob.

From the analysis above, the gob can be categorized into four zones based on its stress characteristics, and the caved strata have no contact with the uncaved strata both in voussoir influencing and pilling zones, as shown in Figure 13, and the compacted and compacting zones are continuously compacted.

The voussoir influencing zone is located at the back of the gob, which is influenced by the voussoir beam formed by the key block of the broken main roof. The length of this zone can be calculated by the following equation:

$$X_v = \frac{L_i + w - L_s}{2}, \tag{7}$$

where L_i is the initial weighting interval, w is the opening width, and L_s is the length of support beam. It is noted that the initial weighting interval can be determined from measurements in the field or from the following equation [3]:

$$L_i = h\sqrt{\frac{2R_T}{q}}, \tag{8}$$

where R_T is the tensile strength of the main roof, and q is the main roof load as imposed by the overlying strata.

Caved strata in the pilling zone are sporadic and not compacted by the main roof and it above. Due to the periodic articulation and instability of the key blocks, the working face causes a weighting when the advancing distance reaches X_h after the last weighting,

$$X_h = L_p, \tag{9}$$

where L_p is the periodic weighting interval that can be determined from measurements in the field or from the following equation [3]:

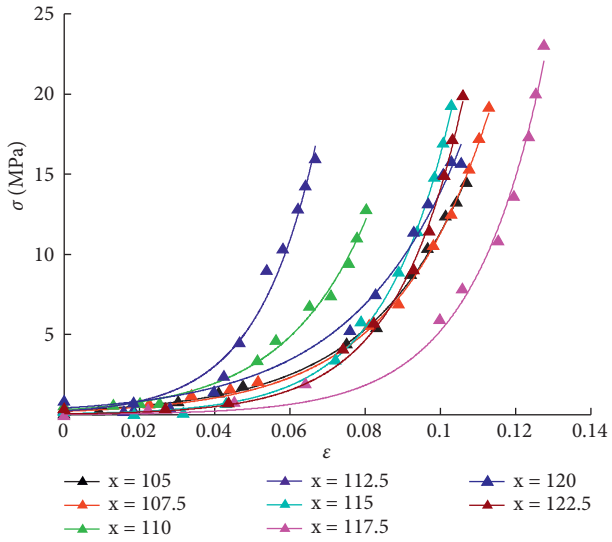

Figure 12: Stress-strain relationship of the gob at different positions.

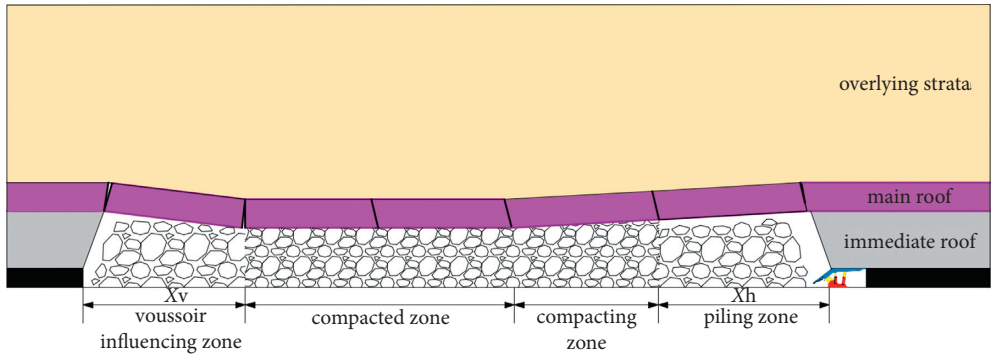

Figure 13: Location of the four zones within the gob area.

Table 3: Coefficients for average height of caving zone [27, 28].

Strata lithology	Compressive strength (σ_c, MPa)	Coefficients	
		c_1	c_2
Strong and hard	>40	2.1	16
Medium strong	20–40	4.7	19
Soft and weak	<20	6.2	32

$$L_p = h\sqrt{\frac{R_T}{3q}}. \tag{10}$$

Therefore, the filling range in advancing direction can be determined from (7) and (9), indirectly. The height of the filling zone can be determined from (11) and Table 3, which are used to estimate the height of the caved zone and were proposed by Bai [27, 28].

$$H_c = \frac{100h}{c_1 h + c_2}. \tag{11}$$

5. Conclusions

The inner force of caved strata is transferred from the mean of the force chain. Both the vertical and horizontal stresses in the longwall gob are nonuniform and jagged. The gob can be categorized into four zones based on its stress characteristics. These are the voussoir influencing zone in the back of the gob, compacted zone, compacting zone, and pilling zone in the front of the gob. The initial bulk factor ranges from 1.12–1.25, which corresponds to a caved zone height that is 4–8 times the mining height. The residual bulk factor is around 1.05. The vertical stress in the compacted zone not

only returns to but exceeds the premining stress, which indicates the compacted zone bears its own overburden in addition to the overburden adjacent to it. However, the horizontal stress only approximately returns to the primitive level. The stress-strain curve has strain hardening behaviour that increases exponentially, and the range of the interaction between the caving strata and the overburden in gob is determined, which provides a basis for determining the gob filling range when using a continuum method to simulate longwall mining.

Data Availability

Some or all data, models, or codes that support the findings of this study are available from the corresponding author upon reasonable request.

Conflicts of Interest

The authors declare that they have no conflicts of interest.

Acknowledgments

The authors gratefully acknowledge the financial support from the Fundamental Research Funds for the Central Universities (2021YQNY10 and 2021YJSNY03).

References

[1] W. Pan, X. Wang, Q. Liu, Y. Yuan, and B. Zuo, "Non-parallel double-crack propagation in rock-like materials under uniaxial compression," *International Journal of Coal Science & Technology*, vol. 6, no. 3, pp. 372–387, 2019.

[2] B. Wang, F. Dang, W. Chao, Y. Miao, J. Li, and F. Chen, "Surrounding rock deformation and stress evolution in predriven longwall recovery rooms at the end of mining stage," *International Journal of Coal Science & Technology*, vol. 6, no. 4, pp. 536–546, 2019.

[3] S. S. Peng, *Coal Mine Ground Control*, Wiley Interscience, New York, NY, USA, 2008.

[4] M. Qian, X. Miao, and J. Xu, "Theoretical study of key stratum in ground control," *Mei Tan Hsueh Pao (Journal of China Coal Society*, vol. 21, 1996.

[5] R. Singh, P. K. Mandal, A. K. Singh, R. Kumar, J. Maiti, and A. K. Ghosh, "Upshot of strata movement during underground mining of a thick coal seam below hilly terrain," *International Journal of Rock Mechanics and Mining Sciences*, vol. 45, no. 1, pp. 29–46, 2008.

[6] B. Unver and N. E. Yasitli, "Modelling of strata movement with a special reference to caving mechanism in thick seam coal mining," *International Journal of Coal Geology*, vol. 66, no. 4, pp. 227–252, 2006.

[7] J. Ju and J. Xu, "Structural characteristics of key strata and strata behaviour of a fully mechanized longwall face with 7.0m height chocks," *International Journal of Rock Mechanics and Mining Sciences*, vol. 58, pp. 46–54, 2013.

[8] Z. Li, J. Xu, J. Ju, W. Zhu, and J. Xu, "The effects of the rotational speed of voussoir beam structures formed by key strata on the ground pressure of stopes," *International Journal of Rock Mechanics and Mining Sciences*, vol. 108, pp. 67–79, 2018.

[9] T. Kuang, Z. Li, W. Zhu et al., "The impact of key strata movement on ground pressure behaviour in the Datong coalfield," *International Journal of Rock Mechanics and Mining Sciences*, vol. 119, pp. 193–204, 2019.

[10] C. Zhang, S. Tu, and Y. Zhao, "Compaction characteristics of the caving zone in a longwall goaf: a review," *Environmental Earth Sciences*, vol. 78, no. 1, p. 27, 2019.

[11] L. Fan and X. Ma, "A review on investigation of water-preserved coal mining in western China," *International Journal of Coal Science & Technology*, vol. 5, no. 4, pp. 411–416, 2018.

[12] W. Li, Q. Wang, S. Liu, and Y. Pei, "Study on the creep permeability of mining-cracked N2 laterite as the key aquifuge for preserving water resources in Northwestern China," *International Journal of Coal Science & Technology*, vol. 5, no. 3, pp. 315–327, 2018.

[13] D. M. Pappas and C. Mark, *Behavior of Simulated Longwall Gob Material*, US Department of the Interior, Bureau of Mines, USA, 1993.

[14] M. G. Karfakis, C. H. Bowman, and E. Topuz, "Characterization of coal-mine refuse as backfilling material," *Geotechnical & Geological Engineering*, vol. 14, no. 2, pp. 129–150, 1996.

[15] M. Li, J. Zhang, N. Zhou, and Y. Huang, "Effect of particle size on the energy evolution of crushed waste rock in coal mines," *Rock Mechanics and Rock Engineering*, vol. 50, no. 5, pp. 1347–1354, 2017.

[16] B. Yu, Z. Chen, Y. Ling, and S Pan, "Particle size distribution and energy dissipation of saturated crushed sandstone under compaction," *J. Min. Saf. Eng*, vol. 35, no. 1, pp. 197–204, 2018.

[17] F. Gao, D. Stead, and J. Coggan, "Evaluation of coal longwall caving characteristics using an innovative UDEC Trigon approach," *Computers and Geotechnics*, vol. 55, pp. 448–460, 2014.

[18] F. Gao, D. Stead, and H. Kang, "Simulation of roof shear failure in coal mine roadways using an innovative UDEC Trigon approach," *Computers and Geotechnics*, vol. 61, pp. 33–41, 2014.

[19] T. D. Le, J. Oh, B. Hebblewhite, C. Zhang, and R. Mitra, "A discontinuum modelling approach for investigation of Longwall Top Coal Caving mechanisms," *International Journal of Rock Mechanics and Mining Sciences*, vol. 106, pp. 84–95, 2018.

[20] I. C. Group, *UDEC User's Guide, Version 6.00*, Itasca Consulting Group, Minnesota, USA, 2018.

[21] J. Wang, Z. Wang, and Y. Li, "Longwall top coal caving mechanisms in the fractured thick coal seam," *International Journal of Geomechanics*, vol. 20, no. 8, 2020.

[22] Z. Guangchao, Z. Chuanwei, C. Miao et al., "Ground response of entries driven adjacent to a retreating longwall panel," *International Journal of Rock Mechanics and Mining Sciences*, vol. 138, Article ID 104630, 2021.

[23] Z. Zhang, J. Bai, Y. Chen, and S. Yan, "An innovative approach for gob-side entry retaining in highly gassy fully-mechanized longwall top-coal caving," *International Journal of Rock Mechanics and Mining Sciences*, vol. 80, pp. 1–11, 2015.

[24] A. Yadav, B. Behera, S. K. Sahoo, G. S. P. Singh, and S. K. Sharma, "An approach for numerical modeling of gob compaction process in longwall mining," *Mining, Metallurgy & Exploration*, vol. 37, no. 2, pp. 631–649, 2020.

[25] Z. Guo, L. Zhang, Z. Ma, F Zhong, J Yu, and S Wang, "Numerical investigation of the influence of roof fracturing angle on the stability of gob-side entry subjected to dynamic loading," *Shock and Vibration*, vol. 2019, Article ID 1434135, 13 pages, 2019.

[26] J. Guo, Y. Li, F. He, G Fu, and S Gao, "Study on stability control of retained gob-side entry by blasting fracturing roof technology in thick immediate roof," *Shock and Vibration*, vol. 2021, Article ID 6613562, 12 pages, 2021.

[27] M. Bai, F. S. Kendorski, and D. Van Roosendaal, *Chinese and North American High-Extraction Underground Coal Mining Strata Behavior and Water protection Experience and Guidelines*, West Virginia University, Morgantown, WV, USA, 1995.

[28] H. Yavuz, "An estimation method for cover pressure re-establishment distance and pressure distribution in the goaf of longwall coal mines," *International Journal of Rock Mechanics and Mining Sciences*, vol. 41, no. 2, pp. 193–205, 2004.